Annals of Nuclear Energy 36 (2009) 567–574

Contents lists available at ScienceDirect

Annals of Nuclear Energy

journal homepage: www.elsevier.com/locate/anucene

Homogeneous zones definition in deterministic codes and effect on computed neutronic parameters

M. Varvayanni [a,*], P. Savva [a], N. Catsaros [a], M. Antonopoulos-Domis [b]

[a] NCSR "DEMOKRITOS", P.O. Box 60228, 15310 Aghia Paraskevi, Attiki, Greece
[b] School of Electrical and Computer Engineering, Aristotle University of Thessaloniki, Thessaloniki, Greece

ARTICLE INFO

Article history:
Received 30 October 2008
Received in revised form 8 January 2009
Accepted 9 January 2009
Available online 23 February 2009

ABSTRACT

The design or modification and in general the analysis and control of nuclear reactors require complex calculations, which are carried out by numerical codes including neutronic and thermal-hydraulic components. Among the neutronic codes, the deterministic ones which solve the neutron transport/diffusion equation simulate the reactor core by dividing it into homogenized zones, i.e. volumes within which the macroscopic nuclear properties are considered uniform. These codes have been extensively used and tested for several decades and are shown to perform well when they analyze reactor cores containing regions with relatively homogeneous distributions of fuel, moderator and absorbing materials. In this work, the sensitivity of computed key neutronic parameters to the partitioning of the reactor core in homogenized zones is examined. Application is made for a configuration of the Greek Research Reactor (GRR-1) core, which is pool type, fueled by slab-type fuel elements. For the calculations, the neutronic code system consisting of XSDRNPM (cell-calculations) and CITATION (core analysis) is used with two different definitions of homogeneous zones for the special/control fuel assemblies. The effect on computations of neutron flux distribution, void-induced reactivity and total control rod worth is examined based on corresponding measurements. It is shown that with a more appropriate partition in homogeneous zones, the agreement of computed results with measurements can be remarkably improved concerning mainly the neutron flux, while the control rods worth is the less affected quantity.

© 2009 Elsevier Ltd. All rights reserved.

1. Introduction

An operating nuclear reactor often undergoes modifications or is planned to host new experimental facilities, actions which require complete core re-analysis with numerical codes including neutronic and thermal-hydraulic predictions. The neutronic codes, which determine the neutron distribution in the core and provide the related parameters for given operating conditions, are distinguished in two main categories, i.e. the deterministic ones which solve the neutron transport equation (or in most cases its diffusion approximation) and those which simulate individual neutron histories and record aspects of their average behavior, using the Monte Carlo methodology. During the last decades, the Monte Carlo codes are widely used because of their capability to treat complex geometries and to represent more accurately the cross-section data by using a continuous energy scale. The Monte Carlo codes include TRIPOLI (Petit et al., 2008), MCNP (Briesmeister, 2000), UNÌC (Palmiotti et al., 2007), PSG (Leppänen, 2005), etc.

The diffusion theory used in the first category codes provides a strictly valid mathematical description of the neutron flux when the assumptions made for its derivation are satisfied. Diffusion codes have been historically proved well suited for the analysis of reactors with relatively homogeneously distributed moderator and neutron source/sink regions. Yet, for modern nuclear reactors consisting of a number of small elements, often highly absorbing, with dimensions of the order of few neutron mean free paths, diffusion codes are still widely used for neutronic analysis and make accurate predictions (Stacey, 2001), being more appropriate for core configurations optimization by offering the advantage of significantly faster execution than Monte Carlo codes, allowing also fast and accurate fuel burn-up calculations. The diffusion codes are based on the definition of homogeneous regions. That is, many small elements in a large region are replaced by a homogenized mixture with effective averaged cross-sections and diffusion coefficients (homogeneous zones), creating thus a computational domain where diffusion theory is valid. Diffusion codes include CITATION (Fowler et al., 1971), DIF3D (Derstine, 1984), APOLLO (Coste et al., 1993), EPISODE (Ikeda and Takeda, 2001), ERANOS (Ruggieri et al., 2006), etc. Diffusion codes typically co-operate with one-dimensional codes for cell-calculations which provide the neutronic properties of the homogenized zones and/or collapse the cross-sections of the fine neutron energy groups into coarse ones. Typical examples are WIMS (Askew et al., 1966), XSDRN (Greene and Petrie, 2000), etc.

* Corresponding author. Tel.: +30 210 650 3720; fax: +30 210 653 3431.
E-mail address: melina@ipta.demokritos.gr (M. Varvayanni).

0306-4549/$ - see front matter © 2009 Elsevier Ltd. All rights reserved.
doi:10.1016/j.anucene.2009.01.009

Although the optimum fuel assembly homogenization techniques are well investigated and applied by experienced neutronic codes users, the corporate experience is not easily available in the open literature. In the present work, one of the later configurations of the Greek Research Reactor Core (GRR-1) is analyzed, using the diffusion code CITATION with the cell-calculations module XSDRN (XSDRNPM version). The analysis of GRR-1 is made for two different partitions of the computational domain into homogenized zones and the results are compared with measurements of thermal neutron flux, control rod worth and void reactivity. Comparison is made between two different zone definitions for the special/control fuel assemblies, regarding the more accurate reproduction of experimental results. It is shown that the neutron flux distribution is very sensitive regarding the method of fuel assembly partitioning into homogenized zones, especially when flux traps and neutron absorbing regions are treated. The selection of an appropriate fuel assembly partitioning also improves, although less significantly than the neutron flux, the computed void-induced reactivity. The sensitivity of the calculated control rods' worth to the fuel assembly partitioning was found almost insignificant.

2. Description of the GRR-1 core

GRR-1 is a pool type, light water moderated and cooled reactor, normally operating at 5 MW. It uses beryllium reflectors, slab-type fuel elements and shim/safety control rods. The GRR-1 core configuration used in the present application is mixed, composed of both HEU and LEU (respectively, High and Low Enrichment in Uranium) fuel assemblies, 28 of which standard and six special. Five of the latter contain a control rod (henceforth called control fuel assemblies) while one is placed near the core center and is used as a flux trap for material irradiation in high fluxes. The fuel assemblies and the beryllium blocks are supported by an aluminum grid plate. The horizontal cross-section (letters in *x*- and numbers in *y*-direction) of the utilized core configuration is shown in Fig. 1.

The dimensions of fuel assembly in *x*, *y* (horizontal) and *z* (vertical) directions are 7.61 cm, 7.956 cm and 62.55 cm, while those of the fuel plate are 6.66 cm, 0.152 cm and 62.55 cm. The latter includes the fuel meat of *x*, *y*, *z* dimensions 6.23 cm, 0.05 cm and 59.65 cm, clad with aluminum of 0.215 cm, 0.051 cm and 1.45 cm thickness in each side of *x*, *y* and *z* directions, respectively. The special/control fuel assembly is composed of 10 fuel plates, five at each side, with a central space where the control rod can be plunged (Fig. 2). The plates that enclose the central space are of aluminum, while the water channel between the aluminum and the adjacent fuel plate is slightly narrower (i.e. 0.27 cm instead of 0.29 cm) than the channel between two successive fuel plates. Fig. 3 shows in detail the geometry of the assembly "basic-cell", contained e.g. between the imaginary lines CD and EF of Fig. 2. In the standard fuel assembly this basic-cell is repeated 18 times without any intermediate interruption. The GRR-1 fuel composition is shown in Table 1.

GRR-1 uses five shim/safety control rods. Their active part has a cross-section of rectangular shape with rounded sides as shown in Fig. 4, while its length equals the active length of the fuel assembly. The absorbers thickness is 0.3575 cm and its material is by weight composed of 82.4% silver (isotopes Ag-107 and Ag-109), 10.7% indium (isotopes In-113 and In-115) and 6.9% cadmium (isotope Cd-113). The absorber composition is shown in (Table 2). The cladding consists of 70% by weight iron, 18% chromium, 10% nickel and 2% manganese.

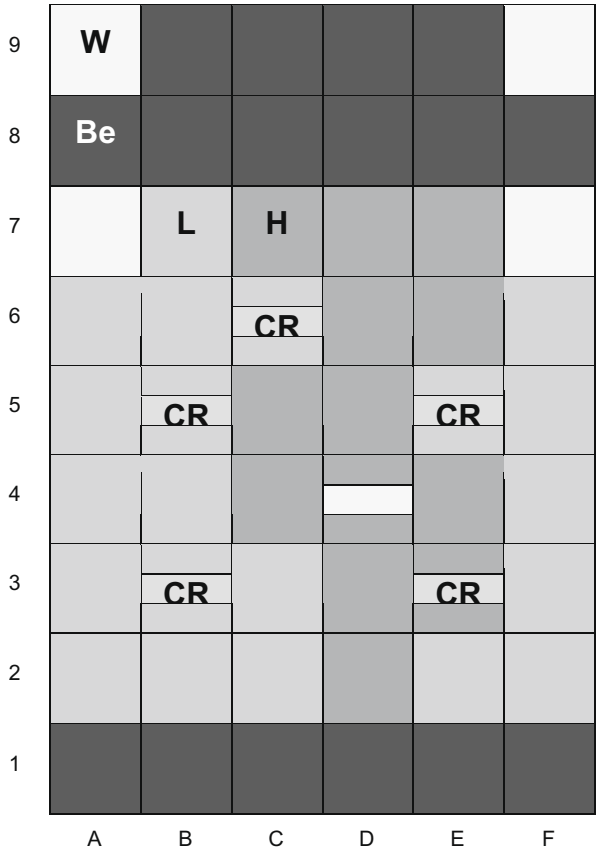

Fig. 1. Horizontal cross-section of the GRR-1 Core. The notation is: **L, H,** for low and high uranium enrichment fuel assemblies, respectively, **CR** for control fuel assemblies with control rods inserted, **W** for water and **Be** for beryllium reflector.

3. Measurements in the GRR-1 core

Three sets of measurements in the GRR-1 have been utilized for comparison with numerical computations in this work. These include measurements of (a) the thermal neutron flux along the D4 core channel at 5 MW power level, (b) the reactivity change with void insertion in the irradiation channel D4 and (c) the five control rods worth.

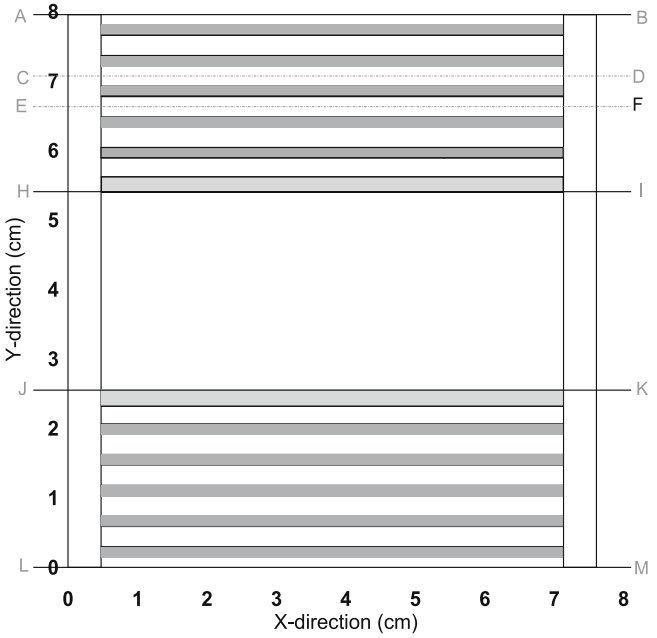

Fig. 2. Cross-sectional area (*x*–*y* dimensions) of the special fuel assembly.

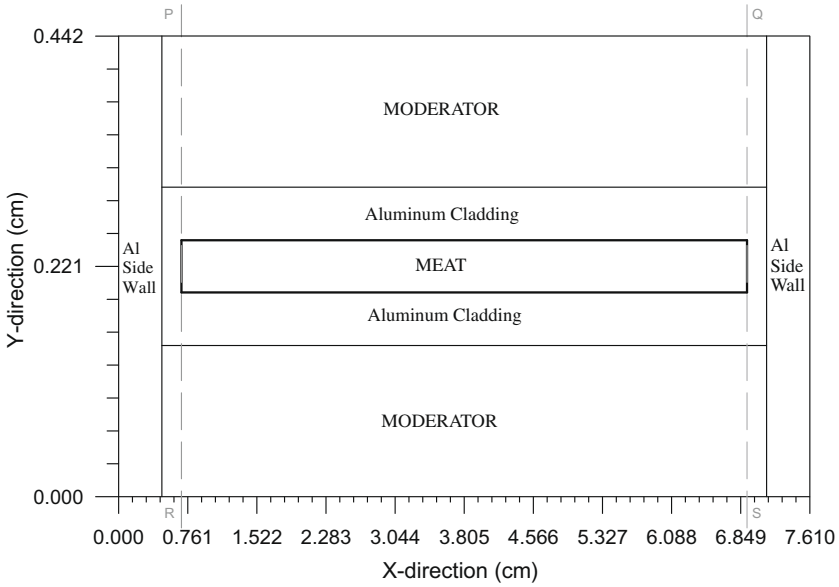

Fig. 3. Cross-sectional area (*x*–*y* dimensions) of the fuel assemblies' basic-cell. The standard fuel assembly is composed of 18 sequential basic-cells, while the special/control contains two opposite parts with five basic-cells each.

Table 1
GRR-1 Fuel composition.

Fuel composition	HEU	LEU
Meat composition	UAl	U_3Si_2–Al
U-235/plate (approx. av.), (g)	10.05	12.34
U-238/plate (approx. av.), (g)	0.75	50.14
Enrichment in U-235 (%)	93	19.75
U-metal/plate (approx. av.), (g)	10.8	62.48
U density in meat (g/cm^3)	0.58	3.36
U-235 density in meat (g/cm^3)	0.54	0.66
Cladding material	Al	Al

3.1. Thermal neutron flux in the D4 flux trap

The thermal neutron flux was experimentally determined by irradiating thin Au foils and by measuring the induced activity of a bare Au-foil and a Cd-covered Au foil of the same dimensions, at each depth of interest. The foils were mounted on aluminum stringers placed at the positions of measurement. Each foil was counted at a calibrated gamma spectrometry set-up consisting of an HPGe detector connected to a CANBERRA 35+ 4k multi-channel analyzer and a suitable software for the peak analysis and the appropriate treatment of the activities to yield the final thermal neutron flux. The measured thermal flux corresponds to neutrons with energy less or equal to 0.5 eV.

3.2. Void induced reactivity in D4 flux trap

The reactivity change due to void insertion was measured by inserting in the D4 core irradiation channel an empty, closed, 8 m-long aluminum tube, with external diameter of 2.5 cm and 0.2 mm thickness. The tube was bent at about its middle length, to avoid neutron streaming and was inserted along the central axis of the rectangular space, in the whole active core depth. The reactor was made critical at 1 kW and the tube was inserted in one stage. The reactor period was measured and the inserted reactivity was estimated based on the measured period, as done for the rod worth measurement (see below).

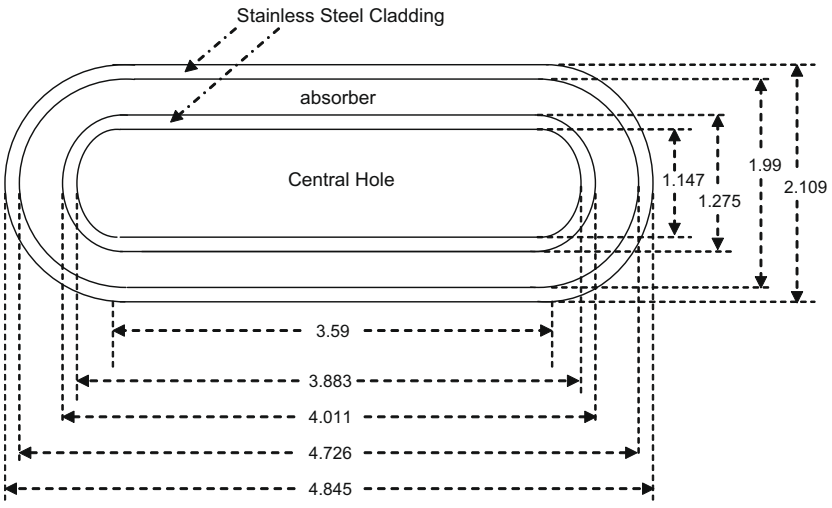

Fig. 4. Cross-section of the control rod. The dimensions are in cm.

Table 2
Control rod absorber composition.

Element	Loading per blade (g)	Isotopes represented	Atom density (atoms/b-cm)
Ag	2100	Ag-107	2.24772×10^{-2}
		Ag-109	2.09042×10^{-2}
In	274	In-113	2.26793×10^{-4}
		In-115	5.06984×10^{-3}
Cd	176	Cd-113	4.25082×10^{-4}

3.3. Control rods worth

For the measurement of a control rod worth, the following procedure was followed. For each control rod to be measured, a compensating rod was defined, typically the most distant from the measured one, so that its displacements would not affect significantly the neutron flux in the vicinity of the measured rod. Initially the examined control rod was fully inserted and the compensating rod was fully withdrawn, while the remaining three rods were kept properly submerged to obtain criticality. The insertion of the three control rods was kept constant during the whole procedure, unless an additional compensating control rod movement was required to maintain criticality. The examined control rod worth was measured by performing successive withdrawals from 100% insertion up to 0% and by recording the reactor period at each step. After each withdrawal of the examined control rod, the compensating rod was properly submerged to balance the inserted reactivity. These steps were repeated until the examined rod was fully withdrawn. At each step, the reactivity change was assessed using the in-hour equation (Stacey, 2001), which expresses the inserted reactivity in terms of the mean life time of the thermal neutrons ℓ, the asymptotic period T, the effective multiplication factor for the critical core ($k_{eff} = 1$) and characteristic parameters of the six delayed neutron groups, such as the fraction of delayed neutrons and the precursor decay constant for each group. The delayed neutron related parameters are found in the literature (e.g. Stacey, 2001) while T was measured and ℓ was known from neutronic calculations for the specific core configuration. The total rod worth was finally obtained by summing the reactivity changes for all successive steps.

4. Calculations for the GRR-1 core

The parameters measured in GRR-1 were computed for the corresponding core configuration, using the neutronics code system XSDRNPM and CITATION. For this purpose, the core is divided in a number of representative cells (usually heterogeneous), which constitute the "zones" in which the cross-sections of the contained materials will be homogenized and collapsed in a number of user-defined neutron energy groups. This is done by XSDRNPM, which provides the collapsed, zone-averaged material cross-sections, based on a master library of fine neutron energy groups. CITATION performs core analysis using the XSDRNPM output with the zone-averaged material concentrations.

4.1. Description of the neutronics code system

XSDRNPM is a module of the SCALE code system that provides one-dimensional cell-calculations and can be used for k_{eff} determination, cross-section collapsing, shielding analysis, and for producing bias factors to use in Monte Carlo shielding calculations. It is a discrete-ordinates code that solves the multigroup, one-dimensional Boltzmann equation in slab, cylindrical, or spherical coordinates. It is primarily an S_n code (utilization of the S_n theory) but includes also options of using the P_1 diffusion theory, the infinite medium theory, or the B_n theory (Greene and Petrie, 2000).

For the GRR-1 applications, XSDRNPM is used for cross-section collapsing. The "cell weighting" option is utilized which is consistent with homogenizing the cross-sections in a heterogeneous cell and is the recommended option to prepare cross-sections for a real reactor analysis with a 3-D reactor model. Cell-weighted cross-sections are defined in a manner that attempts to preserve the reaction rates which occur in the representative cell. The formulation for the assessment of the zone-averaged material cross-section for each defined neutron energy group is given in detail in Greene and Petrie (2000).

CITATION is a three-dimensional code which involves the diffusion approximation of the neutron transport theory, with arbitrary group-to-group scattering. It implements explicit, finite-difference approximations in space, while the neutron-flux-eigenvalue problem is solved by direct iteration to determine the multiplication factor required for a critical system. When a complete outer-iterate set of fluxes is obtained, the eigenvalue is estimated. For the k_{eff} estimation, the overall neutron balance is required. This equation results by summing the point neutron balance equations in a form which causes the outscattering loss of one equation to balance an inscattering source in another equation (Fowler et al., 1971).

CITATION treats cartesian, cylindrical, hexagonal-z and triangular-z geometries. For the GRR-1 core, cartesian coordinates are used. The analyzed volume is divided in parallel layers of different zone-distributions, that is, the vertical core inhomogeneity is described by the parallel layers while the horizontal core inhomogeneity by the layers' zones. Thus, each defined zone has up to two-dimensional geometry, which, in order to be treated by XSDRNPM, must be appropriately transformed to one-dimensional (see Section 4.2). For each zone, a set of zone-average cross-sections is provided by XSDRNPM, collapsed into the defined neutron energy groups for all materials contained in the zone. The set includes the number of neutrons produced per fission and the cross-sections of total absorption, fission, transport, scatter from-group-to-group and a user-selected cross-section, such as (n,α) or $(n,2n)$. Included are also data related to the fission source distribution and energy scatter, as well as nuclide identification data, such as atomic weight, decay constant, useful energy released per fission, etc.

4.2. Application of the neutronics code system to GRR-1 core

For the GRR-1 core analysis with the above described code system, the active reactor core was divided into a proper number of horizontal layers as shown in Table 3. The number N of the intermediate core layers is defined according to the insertion depths of the control rods. Thus, in the general case that the five rods are submerged in different depths, N equals six, i.e. five layers, each one containing at least a slice of one rod and a sixth layer (the lower one) with no rod included. In the present applications $N = 2$ (equal partial insertion of the five rods, or equal deepening of three

Table 3
Definition of horizontal layers in GRR-1 core.

Layer no	Thickness (cm)	Description
1	20.00	Pool-water above core
2	1.45	Upper cladding of fuel element
$3-N$	$Z_3 - Z_N$	Core parts with different insertions of control rods (e.g. all plunged, or some plunged, or none plunged); it holds: $\sum_{i=3}^{N} Z_i = 59.65$ cm
$N+1$	1.45	Down-cladding of fuel element
$N+2$	20.00	Pool-water below the core

rods with the forth one fully inserted and the fifth one fully withdrawn) or $N = 1$ (full rod insertion combined with full rod withdrawal). It is noted that the aluminum supporting grid plate was omitted, since its inclusion has been shown to have insignificant effect on these calculations. The two boundary layers (upper and lower, respectively, numbered 1 and $N + 2$) are homogeneous while all intermediate layers are heterogeneous. Each heterogeneous layer was divided into a number of zones, for cross-sections homogenization by XSDRNPM. The latter was applied with the 238-group NDF5 library, to collapse neutron energy spectrum into five groups (Table 4). The energy boundaries shown are the ones usually selected for the GRR-1 core analysis, so as to define the thermal neutron energy group and the epithermal groups in which rod absorbers have significant absorption cross-sections; for the energy boundaries definition, the requirements of the experimentalists using GRR-1 for irradiations were also taken into account.

Two different zone definitions, named De1 and De2 were considered (Table 5). Each zone is distinguished based on its composition and materials' distribution. Each fuel assembly constitutes a separate zone due to the different fuel burn-up. The zones' geometrical characteristics depend on the selected zone definition. Thus, for both zone definitions the "Std" zone (Table 5) contains the whole cross-sectional area of the standard fuel assembly (i.e. equal 18 times the cross-sectional area of the basic-cell, Fig. 3). The same holds for zones 39 of De1 and 42 of De2. The zone "active part of Spc/Cnt" (Table 5, De1) defines the assembly surface between the imaginary lines AB and HI or equivalently JK and LM (Fig. 2), while the "total Spc" (Table 5, De2) includes the whole assembly surface, between AB and LM (Fig. 2). The zone "total Cnt" (Table 5, De2) is as "total Spc", but in the middle of the central space, a water area is substituted with the control rod (Fig. 4). Similarly, the boundary cladding zone can include either the cladding surface of the active part (De1, zone 40), or the cladding surface of the total assembly with the central space filled with water (De2, zone 43) or filled with control rod (De2, zone 44). Zone 35 of De1 defines the surface between lines HI and JK filled with water (Fig. 2) while zone 36 of De1 includes also the control rod. Finally, zone 41 of De1 is similar to zone 35, but includes also aluminum (tube walls) homogenized with H and O of reduced (due to void insertion) densities. Tube-aluminum and properly reduced H and O densities were also used for zone 45 of De2, where the total, voided assembly in core channel D4, is used as one zone. The core geometry description in CITATION depends on the zones definition. Thus with De1, a core cell that includes a Spc/Cnt assembly, is divided into three parts: the control rod presence in a core horizontal layer is described with zone 36 between two equivalent zones from set 29–34, while the control rod absence is similarly described using zone 35 instead of 36. With De2, the control rod presence in a core cell at a specific level is defined using a zone from set 35 to 39, whereas the rod absence is defined with zones 29–34. Obviously, for a specific core configuration, the number of intermediate core levels (N in Table 3) is the same for De1 and De2.

Each heterogeneous zone contains separate material regions which, for XSDRNPM calculations, must be distributed in one dimension. For this purpose, except for zone 35 of De1 which already has a one-dimensional sequence of different materials (along x-direction), for all other zones the techniques of "extra-zones" definition (tested initially by Papastergiou and Deen, 1981), and/or conversion of heterogeneous material regions to homogeneous by properly averaging the contained material densities, have been utilized. Thus, for zones 1–28 the one-dimensional distribution of material regions was achieved by keeping the material sequence between lines PR and QS (Fig. 3). The materials contained left of PR and right of QS were taken into account through the definition of an extra-zone of specified thickness, shared at both sides of the basic-cell, i.e. below RS and above PQ (Fig. 3). The materials in the extra-zone (Al, H and O) were considered homogeneously distributed, conserving the total mass of each element. An analogous procedure was also followed for zones 29–34, as well as for zones 39 and 40 of De1 and 42 and 43 of De2. One-dimensional geometry for zone 36 of De1 was achieved by converting the control rod surface to circular, conserving the area of each material region; two extra rings were added around the rod surface, one for the water surrounding the rod and one for the aluminum walls that define the control rod channel. For zones 35–39 and 44 of De2, a procedure similar to that for zones 29–34 was followed, with the central part (rod channel) being treated as a region with homogeneous distribution of the contained materials (control rod materials and water). Finally for zone 41 of De1 the one-dimensional structure of zone 35 was kept, considering homogenous distribution of the contained aluminum and water, the latter with reduced density according to its displaced mass. Properly reduced water density mixed with aluminum was also used for zone 45 of De2, in a procedure similar to that followed for zones 35–39 and 44.

Table 4
Upper boundaries of the five collapsed neutron energy groups used.

Energy group	Upper boundary (eV)
5	0.500
4	1.450
3	3.900×10^3
2	7.500×10^5
1	2.000×10^7

Table 5
Definition of homogenized zones. Abbreviations Std, Spc and Cnt stand for the standard, special and control fuel assembly, respectively. Numbers in parentheses give the identification numbers of the different zones in each category.

Core compartments Zone definition De1	Zone definition De2
Std (1–28)	Std (1–28)
Active part of Spc/Cnt (29-34)	Total Spc (29–34)
Central space of Spc (35)	Total Cnt (35–39)
Spc space with control Rod (36)	
Beryllium (37)	Beryllium (40)
Water (38)	Water (41)
Boundary cladding of Std (39)	Boundary cladding of Std (42)
Boundary cladding of active part of Spc/Cnt (40)	Boundary cladding of Spc (43) Boundary cladding of Cnt (44)
Voided central space of Spc (41)	D4 Spc voided in central space (45)

5. Results

5.1. Thermal neutron flux

The computed thermal neutron flux (i.e. for neutron energy group 5, Table 4) along the D4 core channel is shown in Fig. 5, for both zone definitions De1 and De2. As can be seen, definition De1 gives a very good agreement with measurements while De2 underestimates noticeably the thermal neutron flux. This indicates that the representation of the special fuel assembly with three independent zones (fuel-part/flux-trap/fuel-part) reproduces more realistically the thermal neutrons balance (production + thermalization − absorption − leakages) in the assembly's central space.

5.2. Void reactivity

Void reactivity calculations in D4 channel were performed by replacing a water volume equal to the volume of the inserted tube,

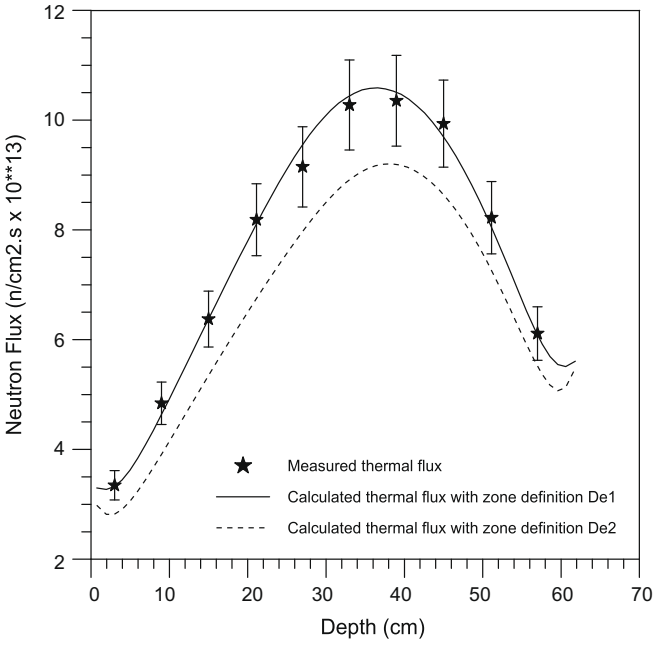

Fig. 5. Thermal neutron flux through the D4 channel of the reactor core, computed for the two zone definitions. Error bars correspond to ±4% error in measurements.

with the aluminum of the tube walls plus the voided tube internal. The results are compared for De1 and De2 in Table 6. Although both methods reproduce satisfactorily the measured void reactivity in D4, De1 gives a very good agreement with measurements; this indicates that the description of the D4 central channel as an independent zone reproduces better the combined result of absorption, moderation and leakage, from which arises the reactivity change. It is noteworthy that despite the gross homogenization of the inserted void, De2 gives higher overestimation of the induced reactivity; this is attributed to the lower D4 thermal neutron flux found with De2, which is related with lower leakages from D4 channel. In fact, if D4 leakages are omitted in the cell-calculations for De2, then the inserted void reactivity is underestimated by more than 40%.

5.3. Control rods worth

Three different approaches, with two stages each, were utilized for the computation of the control rod worth. In each approach two computations of the effective multiplication factor were performed, i.e. k_{eff_0} for the initial and k_{eff_1} for the final stage, while the rod worth was derived from the relationship $\rho_c = (k_{eff\_1} - k_{eff\_0})/k_{eff\_1}$. The following approaches were used: (a) at the first stage all control rods were considered fully withdrawn and at the second the examined rod was fully inserted, (b) at the first stage all control rods were considered fully inserted and at the second the examined rod was fully withdrawn and (c) at the first stage the examined rod was considered fully inserted while the compensating rod fully withdrawn and the remaining rods properly plunged so as to make the reactor critical; at the second stage the examined rod was fully withdrawn while all other rods remained at their initial position. Although only the third set of calculations has a consistency with the experimental procedure, the first two sets were also utilized in order to approach in a more comprehensive way the rod worth and also to assess the code behavior in core environments with different neutron flux distribution (see also below). The results for the five control rods are shown in Table 7 for both De1 and De2. For all computed worths, an uncertainty of about 0.01–0.03% due to the choice of computational parameters (e.g. grid spacing) must be considered.

Comparing computed with experimental results, it should be taken into account that calculations were performed using the nominal (i.e. original, before first irradiation) rod absorber concentrations. However the actual concentrations of the absorbing materials are expected to have undergone a significant depletion, since the control rods in GRR-1 have been used for about 20 years, with an operational scheme of 8 h daily for 5 days a week and approximately 9 months per year, mostly at 5 MW power. During the GRR-1 operation with the studied control rods, several core configurations were operated (e.g. fuel assemblies positioning in more than 6 rows, absence of flux-trap and/or beryllium reflectors, varying relative number and distribution of HEU vs. LEU fuel assemblies). In all cases the control rods R1 and R4 remained close to the core boundary (i.e. first and/or second row of fuel assemblies), at B and E columns, respectively, with absence of beryllium reflectors for the longer operational period. Control rods R3 and R5 were mainly positioned at row 5 and always among HEU fuel assemblies. Rod R2 remained for a long period (about 7 years) next to the core center and after that its position was mainly the one shown in Fig. 1.

Based on the above, an overestimation of most control rods' worth is expected, the magnitude of which depends on the rods historical positioning. Thus, R1 and R4 are expected to be the less depleted control rods, since they have encountered the lower neutron fluxes compared to the other three rods. This explains the relatively low overestimation found between measured and calculated average worth for R1 and R4. On the contrary, control rods R2, R3 and R5 (and mainly R3 and R5) are expected to be the most depleted ones, since their historical positions (i.e. within the HEU fueled region of the core and/or close to the core center) are found in the close vicinity of the higher neutron fluxes in the core. Thus the relatively high overestimation found for the above three rods worth can be considered as reasonable.

The divergence of the results obtained by the three approaches is attributed to the different distribution of the three-dimensional flux computed in the rod vicinity, affecting thus in different manner the obtained rod worth. The changes in the flux distribution are on one hand due to the "rod-shadowing effect", i.e. the flux downgrading in the rod vicinity if neighboring rods are plunged (Bussac and Reuss, 1978) and, on the other hand, to the fact that the neutron flux is normalized by the code in terms of the core power level (Duderstadt and Hamilton, 1976), that is, the three-dimensional neutron flux is distributed so as the total power generated by the core is just the integral of the power density over the core volume. Thus, in the first stage of the first approach (which usually gives the lower rod worth) all rod channels act as flux traps resulting in five (in addition to D4) flux peaks with relatively low values. Therefore, with the rod plunging, the flux drops from a relatively low level. On the contrary, with the second approach

Table 6
Comparison between measured and calculated void reactivity in D4 core position for the two zone definitions. The relative discrepancy is derived from $\Delta(\Delta\rho) = 100(\Delta\rho_c - \Delta\rho_m)/\Delta\rho_c$.

Measured $\Delta\rho_m$ (%$\Delta k/k$)	Calculated $\Delta\rho_c$ (%$\Delta k/k$) De1	Calculated $\Delta\rho_c$ (%$\Delta k/k$) De2	Relative discrepancy (%)	
			De1	De2
6.09×10^{-2}	$6.11\ 10^{-2}$	6.26×10^{-2}	0.3	2.7

Table 7
Comparison between measured and calculated control rod worth for the two zone definitions. The three first rows in each cell of columns 4–7 correspond to the three calculation methods (a), (b) and (c), respectively; the forth row gives the average result. The rods assembly worth and its relative discrepancy are deduced from the average values.

Grid position in core	Studied rod	Measured worth ρ_m (%$\Delta k/k$)	Computed worth ρ_c (%$\Delta k/k$)		Relative discrepancy $(\rho_c - \rho_m)/\rho_c$ (%)	
			De1	De2	De1	De2
B3	R1	2.44	2.22	2.23	−9.91	−9.42
			3.40	3.39	28.24	28.02
			2.35	2.34	−3.83	−4.27
			2.66	**2.65**	**8.27**	**7.92**
B5	R2	1.95	2.31	2.32	15.58	15.95
			2.72	2.70	28.31	27.78
			2.23	2.24	12.56	12.95
			2.42	**2.42**	**19.42**	**19.42**
C6	R3	1.67	2.19	2.18	23.74	23.39
			2.75	2.74	39.27	39.05
			2.15	2.14	22.33	21.96
			2.36	**2.35**	**29.24**	**28.94**
E3	R4	1.84	1.75	1.73	−5.14	−6.36
			2.78	2.74	33.81	32.85
			1.90	1.87	3.16	1.60
			2.14	**2.11**	**14.02**	**12.80**
E5	R5	1.58	1.92	1.89	17.71	16.40
			2.62	2.59	39.69	39.00
			1.93	1.91	18.13	17.28
			2.16	**2.13**	**26.85**	**25.82**
	Rods assembly	9.48	11.75	11.67	19.32	18.77

(which gives the higher values) the thermal flux at the second stage increases noticeably in the emptied rod channel. The third approach is close to the first one, depending each time on the relative plunging of the five rods.

Obviously, since the rod absorbers' depletion cannot be estimated, a direct comparison between measurement and results by methods De1 and De2 cannot be considered. However, one can argue that the two methods give very close results. This is also attributed to the neutron flux normalization in terms of the core power level, so that a flux depreciation in the control rod region is compensated by a flux enhancement in other core regions, as shown for example in (Fig. 6). As can be seen in the same figure, although no measurements exist for comparison, with De1 zones the thermal neutron flux decrease in the control rod is computed significantly stronger than with De2, which again shows the significant effect of the fuel assembly partitioning on the computed neutron flux.

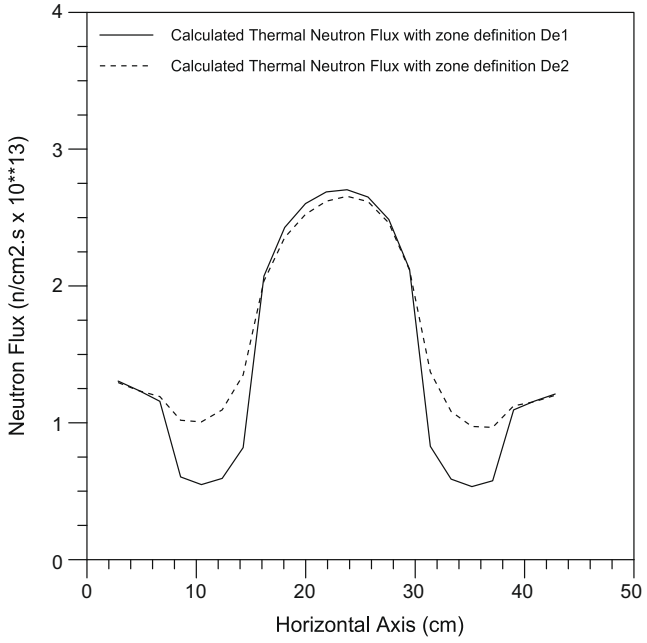

Fig. 6. Thermal neutron flux along the core horizontal row 5. The curves cross the control rods at B5 and E5.

6. Conclusions

Calculations of the thermal neutron flux distribution and the inserted void reactivity along a radiation channel, as well as of the five control rods worth, were made for a later configuration of the GRR-1 core using the neutronics code system XSDRNPM and CITATION. Two different definitions of homogenized zones were used regarding the special/control fuel assemblies and the results obtained were compared with corresponding measurements. It was shown that the consideration of the special/control fuel assembly as a single homogenized zone underestimates the thermal neutron flux along the central space (flux-trap) of the fuel assembly, whereas the division of the assembly into three zones, i.e. "active part/central space/active part" (De1 method) provides a very good agreement with measurements. The De1 fuel assembly partitioning also improves, although less significantly than the neutron flux, the computed void-induced reactivity. The sensitivity of the calculated control rods' worth to the fuel assembly partitioning was found almost insignificant, attributed to the flux normalization in terms of power level.

References

Askew, J.R., Fayers, F.J., Kemshell, F.B., 1966. A general description of the lattice code WIMS. J. Brit. Nucl. Eng. Soc. 5 (4), 564.
Briesmeister, J.-F. (Ed.), 2000. MCNP – A General Monde Carlo N-Particle Transport Code. LA-13709-M. RSICC Computer Code Collection, Oak Ridge National Laboratory, Radiation Safety Information Computational Center, CCC-700. Code available from OECD/NEA Data Bank.
Bussac, J., Reuss, P., 1978. Traité de Neutronique. Hermann, Paris.
Coste, M., Matonnière, G., Sanchez, R., Stankovski, Z., Zmijarevic, I., 1993. APOLLO2, Notice théorique. Rapport DMT/93-581, SERMA/LENR/1535, APOLLO2.
Derstine, K.L., 1984. DIF3D: a code to solve one-, two-, and three-dimensional finite-difference diffusion theory problems. ANL-82-64, Argonne National Laboratory.
Duderstadt, J.J., Hamilton, L.J., 1976. Nuclear Reactor Analysis. Wiley & Sons, Inc., New York.

Fowler, T.B., Vondy D.R., Guningham, G.W., 1971. Nuclear Reactor Core Analysis Code: CITATION. Oak Ridge National Laboratory, ORNL-TM-2496, Rev. 2.

Greene N.M., Petrie, L.M., 2000. XSDRNPM A One-dimensional Discrete-Ordinates Code for Transport Analysis. Oak Ridge National Laboratory, ORNL/NUREG/CSD-2/V2/R6.

Ikeda, H., Takeda, T., 2001. Development and verification of an efficient spatial neutron kinetics method for reactivity-initiated event analyses. J. Nucl. Sci. Technol. 38, 492–502.

Leppänen, J., 2005. A new assembly-level MONTE CARLO neutron transport code for reactor physics calculations. Mathematics and Computation, Supercomputing, Reactor Physics and Nuclear and Biological Applications, Palais des Papes, Avignon, France, September 12–15.

Palmiotti, G., Smith, M., Rabiti, C., Leclere, M., Kaushik, D., Siegel, A., et al., 2007. UNÌC: Ultimate Neutronic Investigation Code. A companion paper in Joint International Topical Meeting on Mathematics and Computation, Supercomputing in Nuclear Applications. Monterey, California, USA, April 15–19.

Papastergiou, C., Deen, J., 1981. Neutronic Calculations for the Conversion of the GRR-1 Reactor from HEU Fuel to LEU Fuel. Unpublished ANL Report, November 1981.

Petit, O., Hugot, F.-X., Lee, Y.-K., Jouanne, C., Mazzolo, A., 2008. Tripoli-4 Version 4 User Guide. Report CEA-R-6169. Code available from OECD/NEA Data Bank.

Ruggieri, J.M., Tommasi, J., Lebrat, J.F., Suteau, C., Plisson-Rieunier, D., De Saint Jean, C., Rimpault, G., Sublet, J.C., 2006. ERANOS 2.1: International code system for GEN IV fast reactor analysis. In: Proceedings of the 2006 International Congress on Advances in Nuclear Power Plants, ICAPP'06, pp. 2432–2439.

Stacey, W.M., 2001. Nuclear Reactor Physics. John Wiley & Sons Inc., New York.